SUPPORTING INFORMATION ONLINE

Ramsden et al.:

Chemoproteomics-based design of potent LRRK2-selective chemical probes that attenuate Parkinson's disease-related toxicity in human neurons

SUPPORTING INFORMATION ITEMS

SI TEXT	Description	relates to
Additional Methods and Synthetic Procedures	Experimental and computational procedures; procedures for compound synthesis	

SI FIGURES	Description	relates to
Fig. S1	A sunitinib-based affinity matrix specifically captures LRRK2 and numerous other kinases from mouse brain and kidney lysate	Figures 1A to D
Fig. S2	Schematic drawing of kinase binding assay	Figures 1 and 2
Fig. S3	A linkable analog of a sunitinib derivative, S7, is an optimized matrix for screening	Figures 1E, 2A and B
Fig. S4	Potency of GW-5074 in recombinant enzyme assay and in binding assay utilizing K562 cell or mouse kidney lysate	
Fig. S5	Viability of rat and human primary cortical neurons in presence of CZC-25146 and CZC-54252	Figure 3

SI TABLES	Description	relates to
Table S1	Overview mass spectrometry experiments	
Table S2	Sequence coverage in LC-MS/MS of LRRK2 captured from mouse brain and kidney	Figure 1B and C
Table S3	Potency of CZC-25146 and CZC-54252 against LRRK2 from mouse brain and kidney lysate	Figure 1E
Table S4	Physicochemical and pharmacokinetic properties of LRRK2 probe compounds CZC-25146 and CZC-54252	

SI DATA SETS	Description	relates to
SI Data Set 1	Compound profiling experiments on la-sunitinib matrix, identification of LRRK2 protein contained in the lower band in kidney	Figure S1C and Table S2
SI Data Set 2	Compound profiling experiments on la-sunitinib matrix: potency and selectivity of sunitinib and S7	Figure 1D
SI Data Set 3	Compound profiling experiments on la-S7 matrix, potency of CZC-25146 and CZC-54252 against LRRK2 from mouse brain and kidney lysate	Table S3, Figure 2C
SI Data Set 4	Selectivity profiling experiments on Kinobeads matrix against i) HeLa, ii) mixed Jurkat, Ramos and iii) mouse brain lysates	Figure 2C

SI Text

Supporting information METHODS

Reagents. If not mentioned otherwise, all reagents were purchased from Sigma. Anti-LRRK2 antibody was purchased from US Biologicals (L4502-20). Secondary antibodies labeled with IRDye®680 and IRDye®800 were from LICOR. Cell lines were purchased from the following suppliers: HeLa (CCL-2), HL-60 (CCL-240), Jurkat E6.1 (TIB-152), Molt-4 (CRL-1582) and Ramos (CRL-1596) from American Type Culture Collection (ATCC), K562 (ACC-10) from German Collection of Microorganisms and Cell Cultures (DSMZ). Cell culture media and supplements were purchased from Invitrogen except for glucose which was purchased by Sigma. NMRI (Naval Medical Research Institute) mouse organs were purchased from Charles River. Sunitinib and GW-5074 were obtained from Sigma or Calbiochem. All other compounds were synthesized in-house as described in Synthetic Procedures in SI Text.

Cell culture and preparation of tissue and cell lysates. HeLa, HL-60, Jurkat E6.1, Ramos and Molt-4 cells were cultured as indicated by the respective suppliers. Frozen mouse organs were quickly thawed at room temperature, then transferred to ice-cold lysis buffer (50 mM Tris-HCl, 0.8% (w/v) Igepal-CA630, 5% (w/v) glycerol, 150 mM NaCl, 1.5 mM $MgCl_2$, 25 mM NaF, 1 mM sodium vanadate, 1 mM DTT, pH 7.5) and homogenized with a rotor stator homogenizer (Polytron homogenizer PT 3100, Kinematica). One complete EDTA-free protease inhibitor tablet (Roche Applied Science) per 25 ml of lysis buffer was added. Frozen cell pellets were homogenized by triturating cells ten times in lysis buffer. Crude lysates were then further dispersed using a dounce homogenizer, kept rotating for 30 minutes at 4° C and spun down for ten minutes at 20,000 x g at 4 °C. The supernatant was spun down again for 1 hour at 145,000 x g. The protein concentration was determined by Bradford assay (BioRad), and aliquots were snap frozen in liquid nitrogen and stored at -80 °C.

Screen for LRRK2 binding compounds. A competition binding assay was performed in 96-well format using 500 µg mouse kidney lysate per data point and 10 µL sepharose beads derivatized with a linkable analog of compound S7 (S7 matrix; 1 mM coupling density). All compounds were diluted to a 50x stock in dimethyl sulfoxide (DMSO) prior to use. Compounds were screened at a final concentration of 3 µM. Each plate contained eight positive (30 µM compound S10) controls; eight negative controls (2 % DMSO) and a dose-response curve for S10 (start concentration of 30 µM, ten dilutions in 1:3 dilution steps). After 2 h binding at 4 °C, the non-bound fraction was removed by washing the beads with lysis buffer. Proteins retained on the beads were eluted in SDS sample buffer (100 mM Tris, 4 % (w/v) SDS, 20 % (w/v) glycerol, 0.00025 % (w/v) bromophenol blue) and spotted on nitrocellulose membranes using an automated liquid dispenser (FluidX). LRRK2 was detected with anti-LRRK2 antibody followed by IRDye®800-labeled antibody for visualization. Fluorescence intensity of individual spots was quantified using a LiCOR Odyssey infrared scanner. Raw integrated intensities in the 800 nm channel were normalized on the raw integrated intensities in the 680 nm channel. Percentage of inhibition was calculated using positive and negative controls, defined as 100 % and 0 % inhibition, respectively. Dose responses for selected

compounds were performed analogously. Curve fitting and IC_{50} determination were done using GraphPad Prism software.

Time-Resolved Fluorescence Resonance Energy Transfer (TR-FRET) LRRK2 kinase assay. The TR-FRET assays for wild type LRRK2 and G2019S mutant were carried out in the following kinase reaction buffer (50 mM HEPES pH 7.5, 10 mM $MgCl_2$, 1 mM EGTA, 2 mM DTT and 0.01 % (w/v) Tween-20). Serially diluted compounds (1 % in DMSO as co-solvent) were pre-incubated with recombinant LRRK2 kinases (Invitrogen) in 384-well Corning black plates at ambient temperature for 15 min. A mixture of ATP and biotin-LRRKtide substrate (Enzo Life Sciences) was subsequently added to the wells at a final concentration of 100 µM and 100 nM, respectively. The final kinase concentration was 5 nM for both wild type LRRK2 and G2019S mutant in 10 µL volume. The kinase reactions were carried out at ambient temperature for 60 min and stopped with the addition of 10 σL/well detection buffer (25 mM HEPES pH7.5, 0.8 mM KF, 40 mM EDTA and 0.1 % BSA) containing europium-conjugated phospho-specific antibody (Cell Signaling; 4 nM) and streptavidin-XL665 (CisBio; 12.5 nM). The plates were read on an Envision plate reader (Perkin Elmer) after 1h incubation, with ratiometric signals (665 nm/615 nm ratio) recorded. The percentage inhibition data were calculated using readings from the control (DMSO) and background (no enzyme) wells. IC_{50} values were determined from the dose-response curves of compounds tested.

LRRK2 binding assay followed by immunoblot. Compound-treated K562 lysates were diluted with lysis buffer without detergent to a final concentration of 0.4 % (w/v) Igepal-CA630. 5 mg diluted lysates were incubated for 1 h at 4 °C with 35 µL S7-matrix, which was then transferred to disposable columns (MoBiTec), washed with lysis buffer containing 0.4 % (w/v) NP-40 and eluted with 50 µl 2x LDS sample buffer (NuPAGE, Invitrogen). Proteins were resolved on a NuPAGE gel (Invitrogen), transferred to PVDF membrane and analyzed for LRRK2 by immune-detection using IRDye®-labeled secondary antibodies and an Odyssey scanner (LiCOR). Data analysis of the quantified bands was performed using Excel and GraphPad Prism software.

Compound profiling and sample preparation for mass spectrometry. Affinity profiling assays were performed as described previously (1) with minor modifications. Derivatized sepharose beads (35 µl of probe matrix per sample) were equilibrated in lysis buffer and incubated with 1 ml (5 mg protein) cell lysate, which had been pre-incubated with test compound or vehicle for 45 min, on an end-over-end shaker for 1 hour. Incubation was done at 4°C for all compounds. Beads were transferred to disposable columns (MoBiTec), washed with lysis buffer containing 0.2 % (w/v) Igepal-CA630 and eluted with 50 µl 2x SDS sample buffer. Proteins were alkylated with 200 mg/mL iodoacetamide for 30 minutes, separated on 4–12 % NuPAGE gels, and stained with colloidal Coomassie Brilliant Blue. Gels were cut into slices across the entire separation range and subjected to in-gel digestion (1). For acquisition of dose-response inhibitor data in one single multiplexed run, TMT (Thermo-Fisher Scientific) tags were used because they allow the acquisition of 6-point data (2). For determination of the identity of the lower LRRK2-immunoreactive band in affinity pull downs from mouse kidney, a maximum of four samples was compared, and iTRAQ reagents (Applied Biosystems) were employed for reasons of economy and coverage (3). Peptide extracts were labeled with iTRAQ or TMT in 40 mM triethylammonium bicarbonate (TEAB), pH 8.53 and the reaction was

quenched with glycine. Labeled extracts were then combined. For compound profiling experiments extracts from vehicle treated samples were labeled with TMT reagent 131, and combined with extracts from compound-treated samples labeled with TMT reagents 126-130. In some cases mixtures of TMT-labeled samples were fractionated using reversed phase chromatography at pH 12 for better peptide coverage, dried and acidified prior to LC-MS/MS analysis (4).

LC-MS/MS analysis. Samples were dried *in vacuo* and re-suspended in 0.1 % formic acid in water and aliquots of the sample were injected into a nano-LC system (Eksigent 1D+) coupled to LTQ-Orbitrap mass spectrometers (Thermo-Finnigan). Peptides were separated on custom 50 cm x 75 µM (ID) reversed phase columns (Reprosil) at 40 °C. Gradient elution was performed from 2 % acetonitrile to 40 % acetonitrile in 0.1 % formic acid over 4 hrs. LTQ-Orbitrap XL and Orbitrap Velos instruments were operated with XCalibur 2.0/2.1 software. Intact peptides were detected in the Orbitrap at 30,000 resolution. Internal calibration was performed using the ion signal from $(Si(CH_3)_2O)_6H^+$ at m/z 445.120025 (5). Data dependent tandem mass spectra were generated for up to six peptide precursors either using PQD (6) or a combined CID/HCD approach (7). For CID up to 5,000 ions (Orbitrap XL) or up to 3,000 ions (Orbitrap Velos) were accumulated in the ion trap within a maximum ion accumulation time of 200 ms. Where indicated targeted data acquisition was used in combination with CID/HCD (8). For HCD target ion settings were 50,000 (Orbitrap XL) and 25,000 (Orbitrap Velos), respectively.

Peptide and protein identification. Mascot 2.0 (Matrix Science) was used for protein identification using 10 ppm mass tolerance for peptide precursors and 0.8 Da (CID) or 20 mDa (HCD) tolerance for fragment ions. Carbamidomethylation of cysteine residues and TMT modification of lysine residues were set as fixed modifications and S,T,Y phosphorylation, methionine oxidation, of proteins and TMT modification of peptide N-termini were set as variable modifications. The search data base consisted of a customized version of the IPI protein sequence database combined with a decoy version of this database created using a script supplied by Matrix Science[7]. Unless stated otherwise, we accepted protein identifications as follows: i) For single spectrum to sequence assignments, we required this assignment to be the best match *and* a minimum Mascot score of 31 *and* a 10x difference of this assignment over the next best assignment. Based on these criteria, the decoy search results indicated <1% false discovery rate (FDR); ii) For multiple spectrum to sequence assignments and using the same parameters, the decoy search results indicate <0.1% false discovery rate. For protein quantification a minimum of 2 sequence assignments matching to unique peptides was required. FDR for quantified proteins was <<0.1%.

Peptide and protein quantification. Centroided TMT reporter ion signals were computed by the XCalibur software and extracted from MS data files using customized scripts. Only peptides unique for identified proteins were used for relative protein quantification and are referred to in supplementary data sets as unique peptide assignments (UPA). Reporter ion intensities were multiplied with the ion accumulation time yielding an area value proportional to the number of reporter ions present in the mass analyzer. For compound competition binding experiments fold changes are reported based on reporter ion areas in comparison to vehicle control and were calculated using sum-based bootstrap algorithm. Fold changes were corrected for isotope purity as described and adjusted for interference

caused by co-eluting nearly isobaric peaks as estimated by the s2i measure (8). Dose-response curves were fitted using R (www r-project.org) and the drc package (www.bioassay.dk) as described previously (1). IC_{50} values were confirmed in replicate experiments using targeted data acquisition (8) for a subset of proteins. Heat maps were created using Tableau software.

Primary rat cortical neuronal culture, neuronal viability and TUNEL assays. (8) All procedures used in this study were approved by the Johns Hopkins Medical Institute Animal Care Committee. The cortex was dissected, incubated for 15 m in in 0.027% trypsin, and then transferred to modified Eagle's medium (MEM)/10% horse serum/10% fetal bovine serum/2 mM glutamine followed by trituration. Dissociated cells were plated at a density of 3-4 $\times$ 10^5 cells per well in polyornithine-coated plates. After 4 days the cells were treated with 10 μg of 5-fluoro-2'-deoxyuridine to prevent proliferation of non-neuronal cells. Cells were maintained in MEM/5% horse serum/2 mM glutamine in 8% CO_2 incubator. The medium was changed twice weekly. For assessment of LRRK2-mediated neuronal injury, LRRK2 and eGFP constructs were combined in a molar ratio of 15:1, respectively, and transfected into neurons with Lipofectamine 2000 (Invitrogen) at DIV (day *in vitro*) 14. On DIV 16, images were collected on a Zeiss Automatic stage with Axiovision 6.0. Viable neurons were defined as having at least one smooth extension (neurite) with twice the length of the cell body. The percentage of eGFP-positive injured neurons in each experimental group relative to those neurons transfected with eGFP was calculated. TUNEL staining was performed as previously described (9, 10) using an *in situ* Cell Death Detection Kit, Red (Roche Molecular Biochemicals). Cells were subjected anti-GFP immunochemical staining, propidium iodide staining and TUNEL staining. Percent viability was calculated by normalizing that data with total eGFP-positive cells in each culture.

Supporting Information SYNTHETIC PROCEDURES

A synthetic procedure for the identification of LRRK2-interacting compounds and for synthesis of a linkable analog of sunitinib has been described elsewhere (11).

Analytical Methods. NMR spectra were obtained on a Bruker dpx400. LC-MS was carried out on an Agilent 1100 using a Gemini C18 (3 x 30 mm, 3 μm bead diameter) column at a 1.2 mL/min flow rate. Solvents used were water and acetonitrile (containing 0.1% formic acid) with an injection volume of 10 μL. Wavelengths for UV analysis were 254 and 210 nm. Gradient:

Time (min)	Water (%)	Acetonitrile (%)
0.0	95	5
3.0	5	95
4.5	5	95
4.6	95	5
5.0	STOP	

Synthesis of key intermediate N-(2-oxoindolin-5-yl) methanesulfonamide

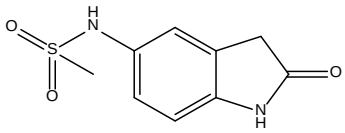

5-aminoindolin-2-one (215 mg) was suspended in dichloromethane (5 mL) and di-isopropylethylamine (1.2 eq, 303 µL) was added. The reaction was cooled in an ice bath and methanesulfonyl chloride (1.1 eq, 123 µL) was added. The reaction was stirred for 1 hour and then allowed to warm to room temperature. The reaction was quenched with a drop of methanol and diluted with ethyl acetate (20 mL). This was then washed with 10 mL aliquots of 2 M hydrochloric acid, water and brine. The organic layer was dried and solvents were removed under reduced pressure.

^{1}H NMR (400 MHz, DMSO) δ 10.39 (s, 1H), 9.35 (s, 1H), 7.10 (s, 1H), 7.09 – 6.98 (m, 1H), 6.79 (d, J = 8.2 Hz, 1H), 3.47 (s, 2H), 2.88 (s, 3H). LC-MS (ES+) 225, RT = 1.05 min

The indolin-2-one intermediate was then used for synthesis of compounds S9 and S10.

General method for the synthesis of S1-S10

A mixture of the indolin-2-one (containing R1 as listed in the table below), the 5-formyl-2,4-dimethyl-1H-pyrrole-3-carboxamide (1eq; containing R2 as listed in the table below)(12, 13), pyrrolidine (catalytic) and ethanol was heated at 100 ^{o}C in a microwave for 30 minutes. The reaction was cooled, diluted with diethyl ether and the precipitate collected by filtration.

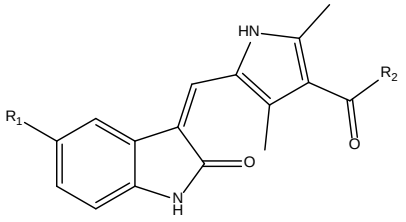

Compound	R1	R2	LC/MS
S1	OCF_3		419 RT= 2.93
S2	OCF_3	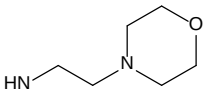	478 RT=2.03
S3	OCF_3	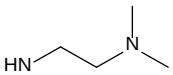	436 RT=2.03
S4	OCF_3	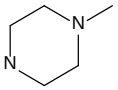	448 RT=2.00
S5	CF_3		403 RT=2.89
S6	CF_3	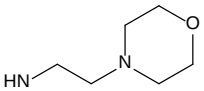	462 RT=2.02
S7	CF_3	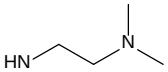	420 RT=2.00
S8	CF_3	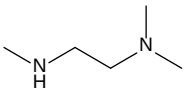	434 RT=2.02
S9	$NHSO_2Me$	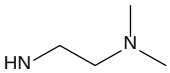	445 RT=1.59
S10	$NHSO_2Me$	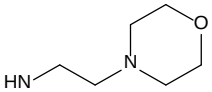	487 RT=0.93

Synthesis of a linkable analog of S7 (la-S7) ((Z)-N-(3-aminopropyl)-2,4-dimethyl-5-((2-oxo-5-(trifluoromethyl) indolin-3-ylidene)methyl)-1H-pyrrole-3-carboxamide hydrochloride

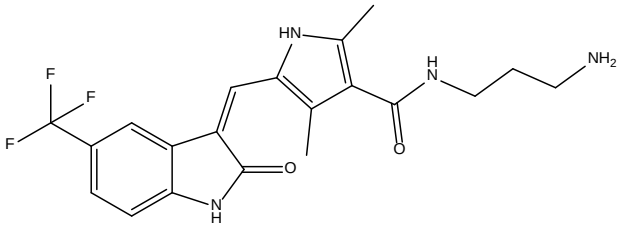

A mixture of 5-(trifluoromethyl) indolin-2-one (530 mg), tert-butyl (3-(5-formyl-2,4-dimethyl-1H-pyrrole-3-carboxamido)propyl)carbamate (852 mg)(11), pyrollidine (100 µL) and ethanol (12 mL) was heated at 100 ^{o}C in a microwave for 30 minutes. The reaction was cooled, diluted with diethyl ether and the precipitate collected by filtration. The residue was suspended in methanol (2.5 mL) and dichloromethane (7.5 mL). 4 M HCl in dioxane (2 mL) was added slowly over 10 minutes to give a clear solution. The reaction was allowed to stand for a further 4 h and the resultant precipitate was collected by filtration and washed with dichloromethane (2 x 10 mL) then dried *in vacuo* to give the product as the hydrochloride salt. Synthesis of an analogous linkable analog of compound S10 yielded a poorly soluble product that was not suitable for immobilization on a solid phase matrix.

1H NMR (400 MHz, DMSO) δ 13.66 (s, 1H), 11.32 (s, 1H), 8.31 (s, 1H), 8.11 – 7.75 (m, 4H), 7.46 (d, J = 8.1 Hz, 1H), 7.05 (d, J = 8.1 Hz, 1H), 3.46 – 3.23 (m, 2H), 3.17 (s, 9H), 2.84 (dd, J = 13.2, 6.7 Hz, 2H), 1.89 – 1.70 (m, 2H).

LCMS (ES+) 405, RT = 1.97 min

Synthesis of intermediate N1-(2-chloro-5-fluoropyrimidin-4-yl)benzene-1,2-diamine

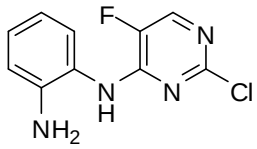

A mixture of 2,4-dichloro-5-fluoropyrimidine (10.0 g, 0.06 mol), *o*-phenylene diamine (7.1 g, 0.066 mol) and DIPEA (20.8 mL, 0.12 mol) in n-butanol (80 mL) were stirred at 110 °C for 16 h then concentrated *in vacuo* then slurried with 0.1 M hydrochloric acid (20 mL). The solid was collected at the pump, washed with water (2 x 20 mL), n-butanol (30 mL) and diethyl ether (2 x 30 m L), then dried under vacuum to afford N1-(2-chloro-5-fluoropyrimidin-4-yl)benzene-1,2-diamine as a colourless powder (10.8 g, 71 %). ^{1}H NMR (d_6-DMSO) δ 9.31 (brs, 1H), 8.18 (d, 1H), 6.99-7.03 (m, 2H), 6.74-6.76 (m, 1H), 6.54-6.58 (m, 1H), 5.04 (brs, 2H); LCMS (ES+) 240, RT = 1.90 min.

Synthesis of intermediate N-(2-(2-chloro-5-fluoropyrimidin-4-ylamino)phenyl)methanesulfonamide

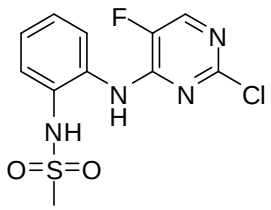

A solution of N1-(2-chloro-5-fluoropyrimidin-4-yl)benzene-1,2-diamine (1.5 g, 6.30 mmol) in pyridine (15 mL) was cooled to 0 ^{o}C before drop wise addition of methanesulfonyl chloride (0.54 mL, 6.93 mmol). The resultant solution was allowed to wam to room temperature and stirred for 18 h. The mixture was diluted with H_2O (25 mL) and EtOAc (25 mL) the organic layer was collected and washed with 2 M hydrochloric acid (2 x 25 mL), brine (25 mL) and dried ($MgSO_4$). It was then concentrated *in vacuo* to provide N-(2-(2-chloro-5-fluoropyrimidin-4-ylamino)phenyl)methanesulfonamide as a beige solid (1.45 g, 72 %). ^{1}H NMR (d_6-DMSO) δ 9.41 (brs, 1H), 9.25 (s, 1H), 8.30 (d, 1H), 7.47-7.52 (m, 2H), 7.32 (t, 1H), 7.25 (t, 1H), 2.99 (s, 3H) ; LCMS (ES+) 316, RT = 2.26 min.

Synthesis of the screening hit N-(2-(2-(2-ethoxy-4-morpholinophenylamino)-5-fluoropyrimidin-4-ylamino) phenyl) methanesulfonamide hydrochloride

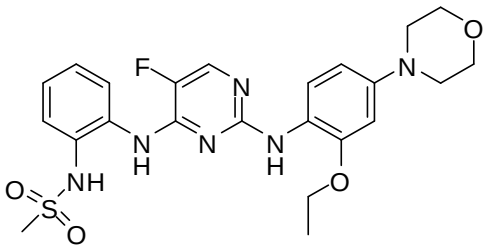

N-(2-(2-chloro-5-fluoropyrimidin-4-ylamino)phenyl)methanesulfonamide (101 mg, 0.32 mmol) and 2-ethoxy-4-morpholinoaniline bis HCl salt (94 mg, 0.32 mmol) were suspended in ethanol (1 mL) and 4 M hydrochloric acid in dioxan (50 µL). The reaction was heated in a microwave at 160 ^{o}C for 45 minutes, was allowed to stand for 1 hour and the precipitate was collected by filtration. The residue was washed with ethanol (1 mL) and ethyl acetate (2 x 1 mL), and then dried *in vacuo* to give the title compound as a brown solid.

^{1}H NMR (d_6-DMSO) δ 7.95 (d, 1H), 7.84 (d, 1H), 7.80 (d, 1H), 7.45 (s, 1H), 7.43 (d, 1H), 7.31 (t, 1H), 7.25 (s, 1H), 6.45 (s, 1H), 6.32 (d, 1H), 4.03 (q, 2H), 3.84 (t, 2H), 3.05, (t, 2H), 2.90 (s, 3H), 1.40 (t, 3H); LCMS (ES+) 503 RT = 2.41 min

Synthesis of CZC-25146 [N-(2-(2-(2-methoxy-4-morpholinophenylamino)-5-fluoropyrimidin-4-ylamino) phenyl) methanesulfonamide hydrochloride]

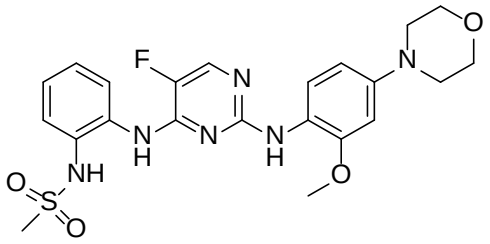

N-(2-(2-chloro-5-fluoropyrimidin-4-ylamino)phenyl)methanesulfonamide (72 mg, 0.23 mmol) and 2-methoxy-4-morpholinoaniline bis HCl salt (64 mg, 0.23 mmol) were suspended in ethanol (1 mL) and 4 M hydrochloric acid in dioxan (50 µL). The reaction was heated in a microwave at 160 °C for 45 minutes. The reaction was allowed to stand for 1 hour and the precipitate collected by filtration. The residue was washed with ethanol (1 mL) and ethyl acetate (2 x 1 mL), then dried *in vacuo* to give the title compound as a brown solid.

1H NMR (400 MHz, DMSO) δ 8.59 (s, 1H), 8.04 (d, J = 3.4 Hz, 1H), 7.87 (dd, J = 7.6, 1.6 Hz, 1H), 7.58 (m, 2H), 7.38 (dd, J = 7.4, 1.8 Hz, 1H), 7.20 (m, 2H), 6.60 (d, J = 2.0 Hz, 1H), 6.35 (dd, J = 8.7, 2.0 Hz, 1H), 3.77 (s, 3H), 3.73 (m, 4H), 3.05 (d, J = 4.4 Hz, 4H), 2.91 (s, 3H). LCMS (ES+) 488, RT=1.92 min.

Synthesis of CZC-54252 [N-(2-((5-chloro-2-((2-methoxy-4-morpholinophenyl)amino)pyrimidin-4-yl)amino) phenyl)methanesulfonamide hydrochloride]

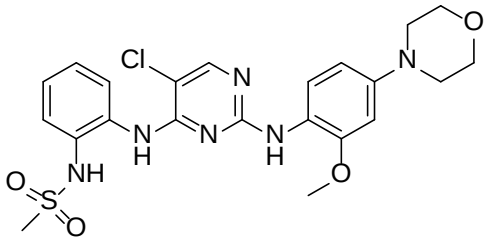

N-(2-((2,5-dichloropyrimidin-4-yl)amino)phenyl)methanesulfonamide(14) (333 mg, 1.00 mmol) and 2-methoxy-4-morpholinoaniline bis HCl salt (280 mg, 1.00 mmol) were suspended in ethanol (2 mL) and 4 M hydrochloric acid in dioxan (100 µL). The reaction was heated in a microwave at 160 °C for 45 minutes. The reaction was allowed to stand for 1 hour and the precipitate collected by filtration. The residue was washed with ethanol (1 mL) and ethyl acetate (2 x 1 mL), then dried *in vacuo* to give the title compound as a brown solid.

The hydrochloride salt was converted to the free base by dissolving in 2 mL of water and neutralising with saturated aqueous sodium hydrogen carbonate. The product was collected by filtration, washed with water and dired in vacuo to give a cream solid.

1H NMR (400 MHz, DMSO) δ 8.51 (s, 1H), 8.08 (s, 1H), 7.99 (d, J = 7.2 Hz, 1H), 7.91 (s, 1H), 7.44 (d, J = 8.6 Hz, 1H), 7.34 (dd, J = 7.6, 1.8 Hz, 1H), 7.25 – 7.10 (m, 2H), 6.61 (d, J = 2.5 Hz, 1H), 6.37 (dd, J = 8.8, 2.5 Hz, 1H), 3.83 – 3.70 (m, 7H), 3.17 – 3.02 (m, 4H), 2.93 (s, 3H). LCMS (ES+) 505, RT=2.18 min.

REFERENCES FOR SUPPORTING INFORMATION

1. Bantscheff M*, et al.* (2007) Quantitative chemical proteomics reveals mechanisms of action of clinical ABL kinase inhibitors. (Translated from eng) *Nat Biotechnol* 25(9):1035-1044 (in eng).
2. Bantscheff M*, et al.* (2011) Chemoproteomics profiling of HDAC inhibitors reveals selective targeting of HDAC complexes. *Nat Biotechnol* 2011 Jan 23. [Epub ahead of print].
3. Thingholm TE, Palmisano G, Kjeldsen F, & Larsen MR (2010) Undesirable charge-enhancement of isobaric tagged phosphopeptides leads to reduced identification efficiency. (Translated from eng) *Journal of proteome research* 9(8):4045-4052 (in eng).
4. Kruse U*, et al.* (2010) Chemoproteomics-based kinome profiling and target deconvolution of clinical multi-kinase inhibitors in primary chronic lymphocytic leukemia cells. (Translated from eng) *Leukemia* 25(1):89-100 (in eng).
5. Olsen JV*, et al.* (2005) Parts per million mass accuracy on an Orbitrap mass spectrometer via lock mass injection into a C-trap. (Translated from eng) *Mol Cell Proteomics* 4(12):2010-2021 (in eng).
6. Bantscheff M*, et al.* (2008) Robust and sensitive iTRAQ quantification on an LTQ Orbitrap mass spectrometer. (Translated from eng) *Mol Cell Proteomics* 7(9):1702-1713 (in eng).
7. Kocher T*, et al.* (2009) High precision quantitative proteomics using iTRAQ on an LTQ Orbitrap: a new mass spectrometric method combining the benefits of all. (Translated from eng) *Journal of proteome research* 8(10):4743-4752 (in eng).
8. Savitski MM*, et al.* (2010) Targeted Data Acquisition for Improved Reproducibility and Robustness of Proteomic Mass Spectrometry Assays. (Translated from Eng) *J Am Soc Mass Spectrom* (in Eng).
9. West AB*, et al.* (2007) Parkinson's disease-associated mutations in LRRK2 link enhanced GTP-binding and kinase activities to neuronal toxicity. (Translated from eng) *Hum Mol Genet* 16(2):223-232 (in eng).
10. Smith WW*, et al.* (2006) Kinase activity of mutant LRRK2 mediates neuronal toxicity. (Translated from eng) *Nat Neurosci* 9(10):1231-1233 (in eng).
11. Drewes G, Hopf C, & Reader V (2009) METHODS FOR THE IDENTIFICATION OF LRRK2 INTERACTING MOLECULES AND FOR THE PURIFICATION OF LRRK2. *Patent No. US2009220992*
12. Shenoy N & Sorasuchart W (2001) Preparation of pyrrole substituted 2-indolinones as antitumor agents. . *PCT Int. Appl. (Sugen, Inc., USA).* CODEN: PIXXD2 WO 2001037820
13. O'Farrell AM & Cherrington J (2003) Treatment of acute myeloid leukemia with indolinone compounds, and preparation thereof. . *PCT Int. Appl. (Sugen, Inc., USA)* CODEN: PIXXD2 WO 2003035009 A2.
14. Major J*, et al.* (2009) Preparation of N-(pyrimidinylaminophenyl) sulfonamides as ZAP-70 inhibitors. *PCT Int. Appl. (Cellzome Ltd., UK)* CODEN: PIXXD2 WO 2009112490 A1.

Suppl. Fig. 1

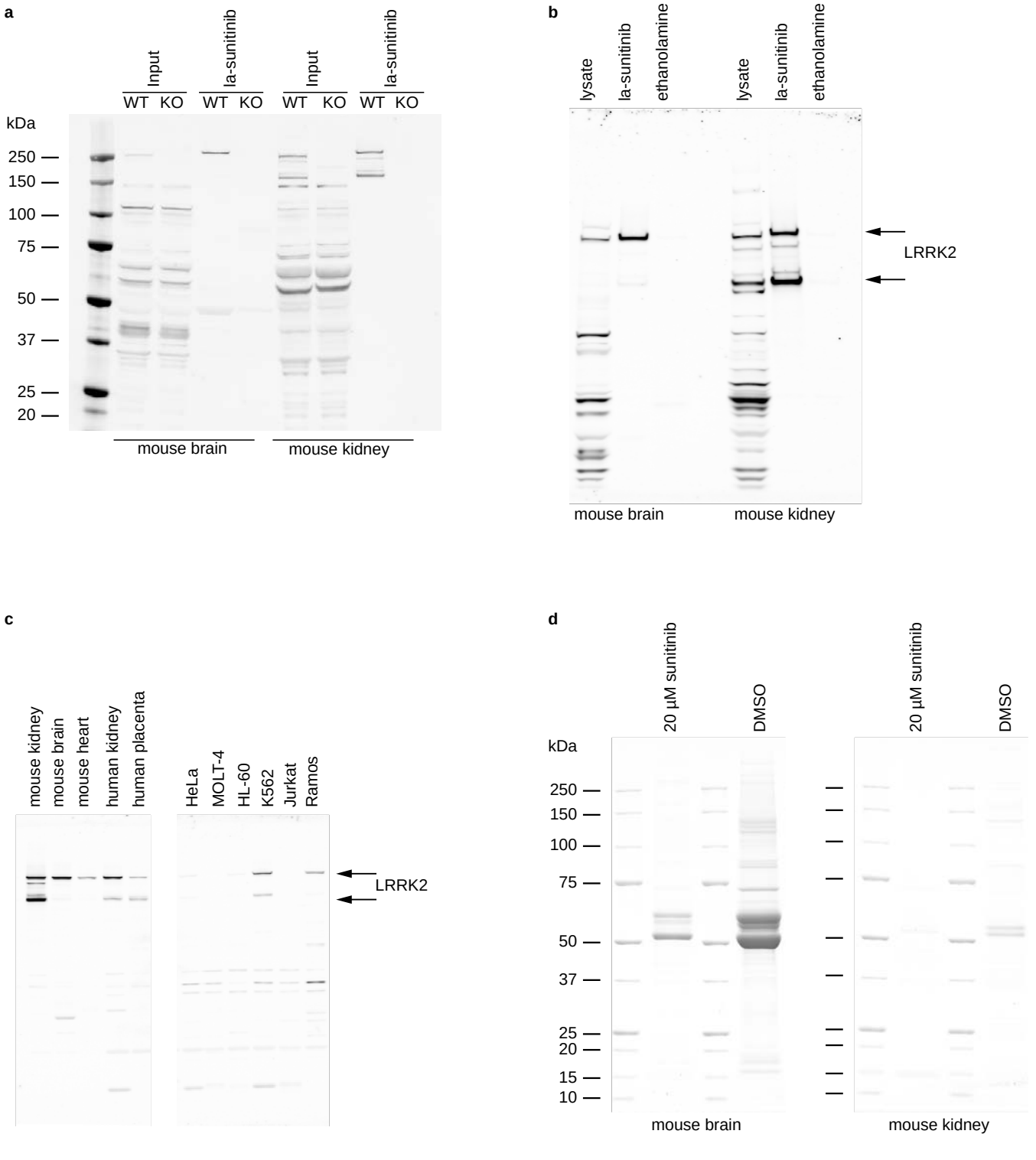
a
Input
la-sunitinib
Input
la-sunitinib
WT KO WT KO WT KO WT KO
kDa
250
150
100
75
50
37
25
20
mouse brain
mouse kidney
b
lysate
la-sunitinib
ethanolamine
lysate
la-sunitinib
ethanolamine
LRRK2
mouse brain
mouse kidney
c
mouse kidney
mouse brain
mouse heart
human kidney
human placenta
HeLa
MOLT-4
HL-60
K562
Jurkat
Ramos
LRRK2
d
20 µM sunitinib
DMSO
20 µM sunitinib
DMSO
kDa
250
150
100
75
50
37
25
20
15
10
mouse brain
mouse kidney

Figure S1 A sunitinib-based affinity matrix specifically captures LRRK2 from mouse brain and kidney lysate.

a) Immunoreactivity captured by la-sunitinib matrix is LRRK2. Full immunoblot representation of **Figure 1b**.

b) la-sunitinib specifically captures isoforms of LRRK2 from mouse brain and kidney extracts. la-sunitinib (or ethanolamine) was coupled to Sepharose matrix and incubated with detergent extract from mouse brain or kidney. Eluted proteins were analyzed by immunoblot with anti-LRRK2 antibody. Molecular weights markers of 250 kDa, 150 kDa and 100 kDa are indicated.

c) la-sunitinib captures LRRK2 from various human and mouse cell and tissue sources. Full immunoblot representation of **Figure 1c**.

d) Proteins are specifically captured by la-sunitinib matrix. Preincubation of mouse brain and kidney lysates with 20 µM sunitinib prevents binding of most proteins to la-sunitinib matrix as assessed by Coomassie staining and LC-MS/MS (**SI Data Set 1**). In analogy to immunoblot results, LRRK2 was detected in two major bands in kidney pull-downs by quantitative LC-MS/MS. Sequence coverage of identified LRRK2 peptides suggests that the LRRK2 in the lower band is an N-terminally truncated fragment (**Table S2**). LRRK1 was not identified in any chemical proteomics experiment.

Suppl. Fig. 2

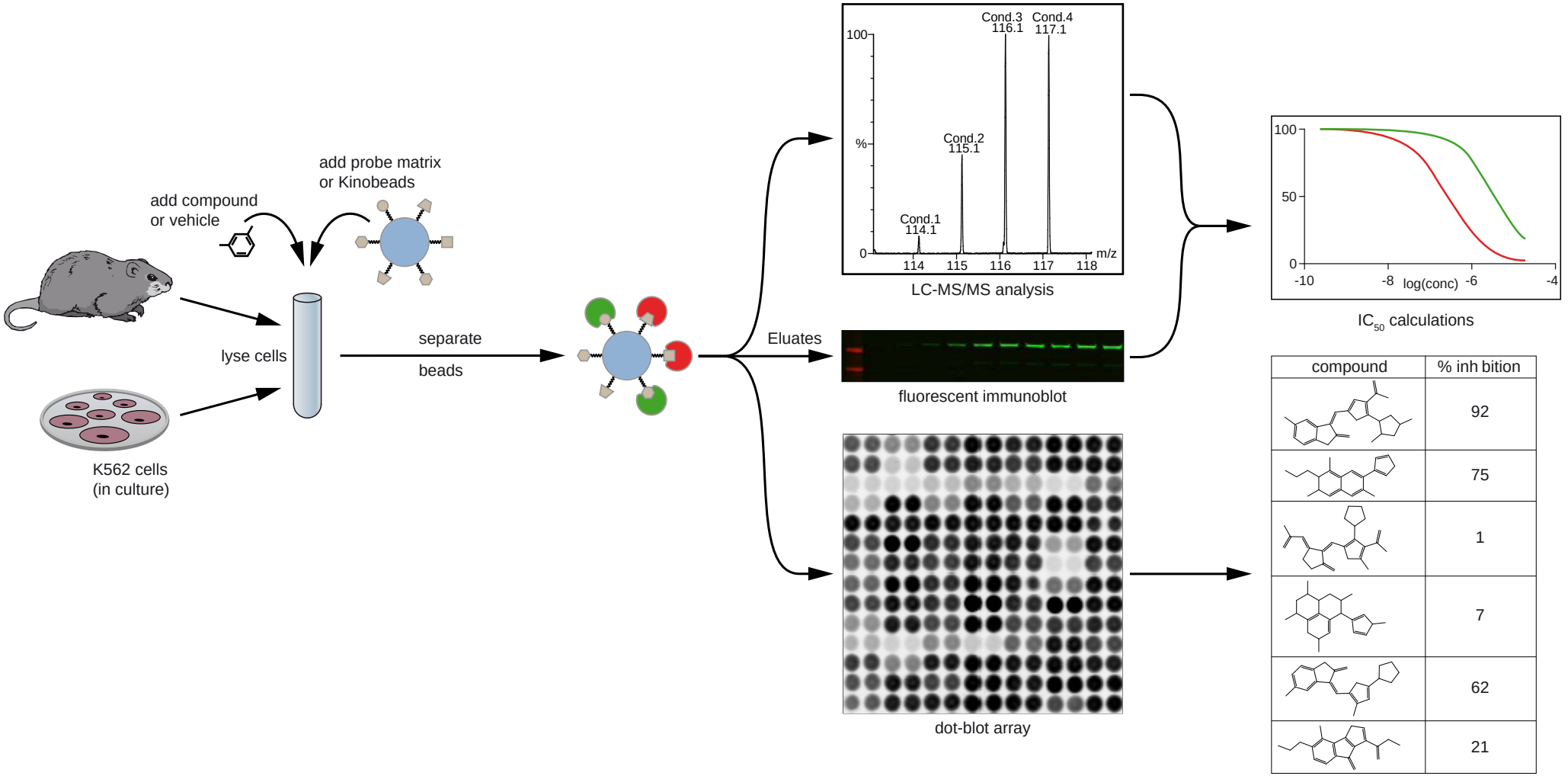
add compound
or vehicle
add probe matrix
or Kinobeads
lyse cells
K562 cells
(in culture)
separate
beads
Eluates
Cond.1
114.1
Cond.2
115.1
Cond.3
116.1
Cond.4
117.1
100
%
0
114
115
116
117
118
m/z
LC-MS/MS analysis
fluorescent immunoblot
dot-blot array
100
50
0
-10
-8
log(conc)
-6
-4
IC50 calculations
compound
% inh bition
92
75
1
7
62
21

Figure S2 Two approaches for chemoproteomics-based assays used for screening, dose-response data and selectivity profiling

Cultured cells or mouse tissues are lysed and extracts are incubated with free test compound (or vehicle control) and a suitable probe matrix. Targets of the immobilized probe compounds that are NOT occupied by free test compound in the lysate are subsequently captured by the probe matrix. Bound kinases are eluted and quantified in various ways: i) by labeling with isobaric TMT™ or iTRAQ™ mass tags (**SI Text Methods**), followed by quantitative LC-MS/MS, for simultaneous determination of concentration-response curves for >100 captured kinases; ii) by quantitative immunoblotting with fluorescent secondary antibodies; iii) by measurement of fluorescence intensity on dot-blot arrays.

Suppl. Fig. 3

a

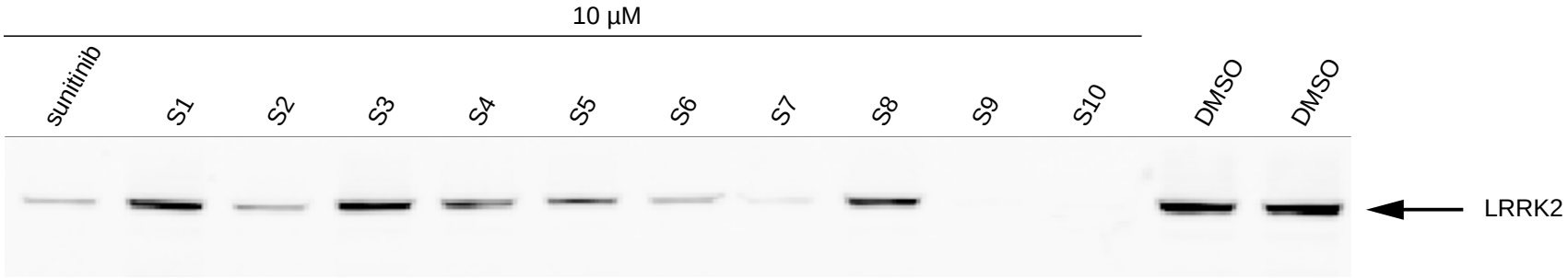

b

Compound	Structure	% inhibition at 10 µM	Compound	Structure	% inhibition at 10 µM
sunitinib	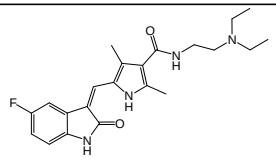	92	S6	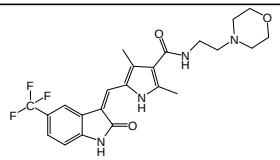	91
S1	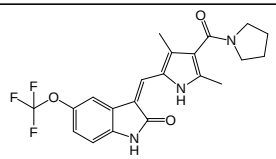	42	S7	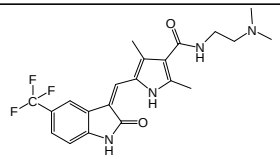	97
S2	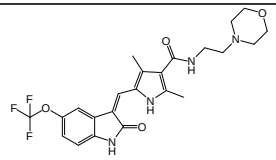	88	S8	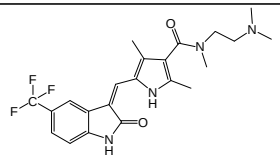	60
S3	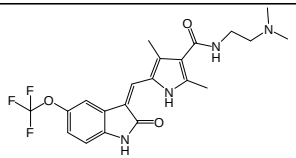	32	S9	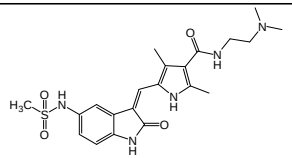	100
S4	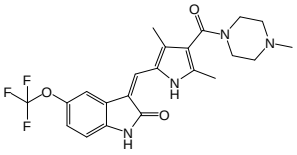	69	S10	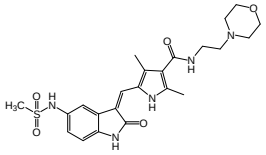	99
S5	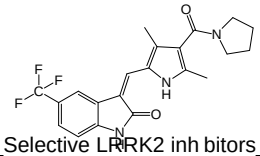	79	LA - S7	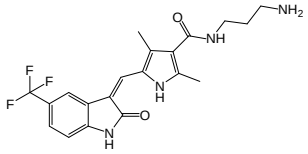	n.d.

Figure S3 A linkable analog of a sunitinib derivative, S7, is an optimized matrix for screening

Ten sunitinib analogs (S1 to S10) were synthesized. Each of them, as well as sunitinib and DMSO as solvent control, were incubated with mouse brain lysate.

a) Following capturing with la-sunitinib matrix, bound proteins were eluted in SDS-PAGE sample buffer and analyzed by immunoblotting with anti-LRRK2 and fluorescent secondary antibody.

b) Fluorescent signals corresponding to inhibition of LRRK2 binding to the probe matrix by S1 to S10 were quantified using an Odyssey scanner. Synthesis of linkable analogs of S9 and S10 was unsuccessful. Therefore, a linkable analog of S7 (la-S7) was synthesized and a kinase focused library of 127 compounds was screened using la-S7 matrix in the dot-blot array format (**Fig. S2**).

a

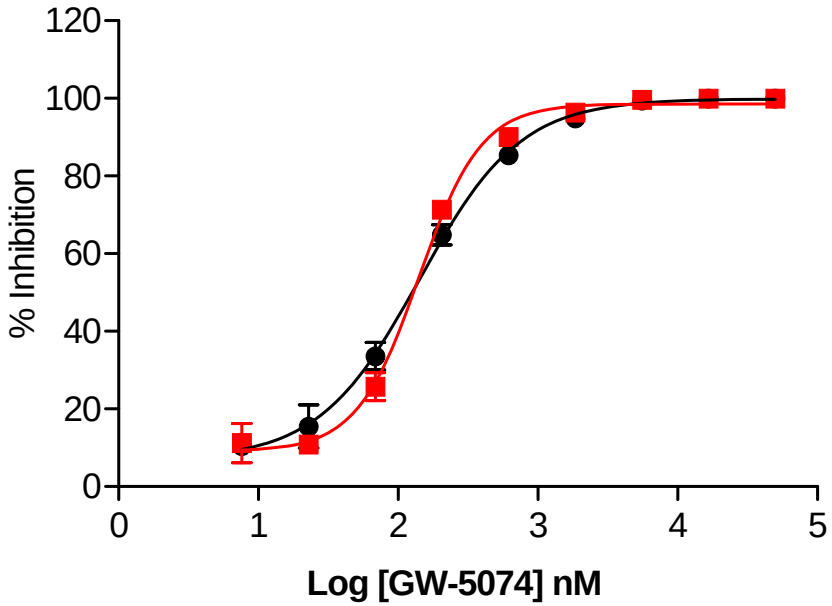

	WT	G2019S
IC_{50}	142.3	140.9

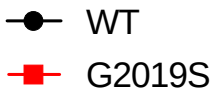

b

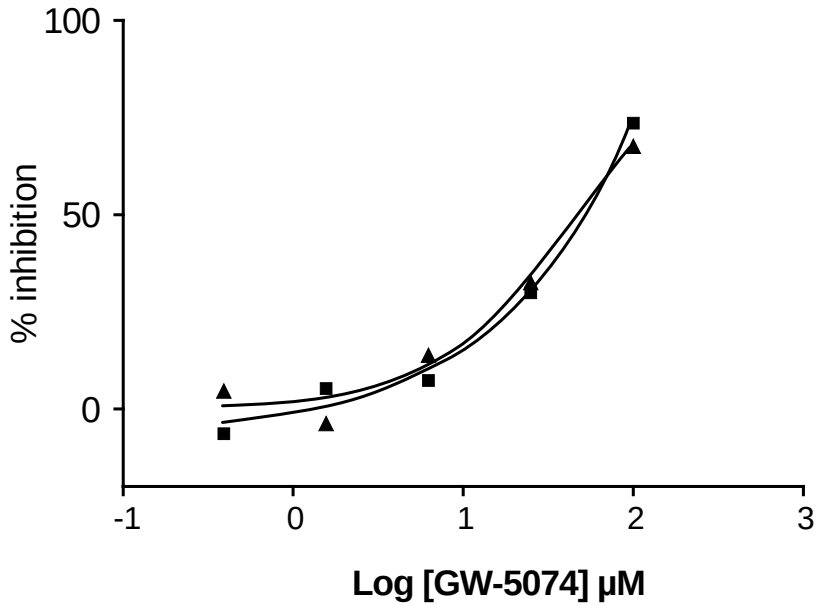

Figure S4 Potency of GW-5074 in recombinant enzyme assay and in binding assay utilizing K562 cell extract

a) For comparison, GW-5074 was tested in the same TR-FRET assay that was used for CZC-25146 and CZC-54252 (**Figure 2a, b**). b) GW-5074 displayed a surprisingly low potency in the la-S7 binding assay with mouse kidney and K562 cell lysate (incomplete curves with concentrations up to 100 μM).

Suppl. Fig. 5

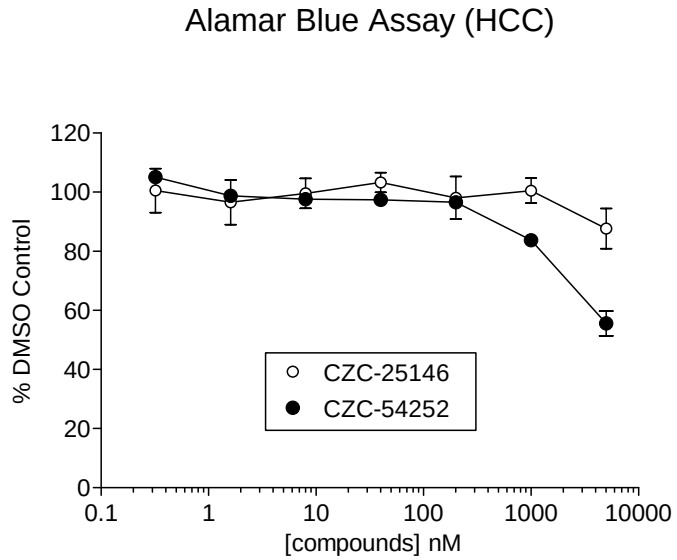
Alamar Blue Assay (HCC)
% DMSO Control
120
100
80
60
40
20
0
0.1
1
10
100
1000
10000
[compounds] nM
CZC-25146
CZC-54252

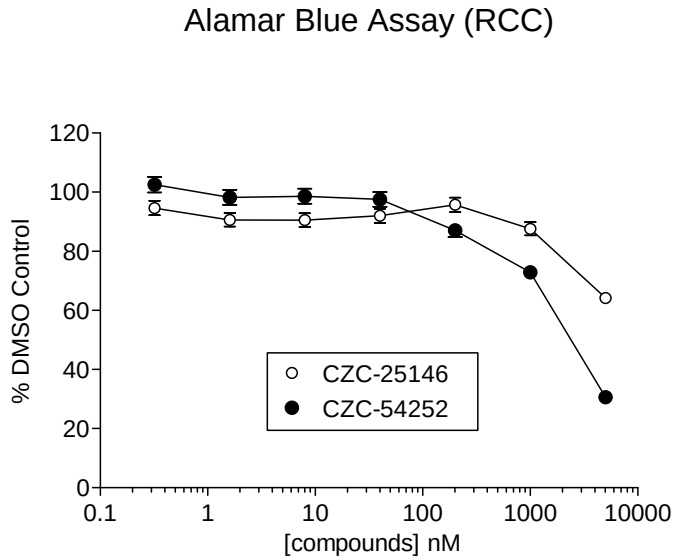
Alamar Blue Assay (RCC)
% DMSO Control
120
100
80
60
40
20
0
0.1
1
10
100
1000
10000
[compounds] nM
CZC-25146
CZC-54252

Figure S5 Cytotoxicity assessment of CZC-25146 and CZC-54252 in rat and human cortical neurons

Primary rat and human cortical cultures were treated with either inhibitor for 6 days and subjected to AlamarBlue assay. CZC-25146 and CZC-54252 showed apparent cytotoxicity at 5 μM and >1 μM, respectively, in the rat cortical culture. A similar but milder effect was observed for the human cortical neurons.

Table S1:

Experiment Overview

VC = vehicle control

Compound concentrations in compound profiling experiments are given in µM										
Compound profiling experiments on sunitinib matrix, identification of LRRK2 protein contained in the lower band in kidney; data for Figure S1C and Table S2										
							compound concentrations [µM]			
experiment ID	**SI data set number**	**probe matrix**	**compound for competition**	**lysate material**	**MS method**	**isobaric tags**	**iTRAQ 114**	**iTRAQ 115**	**iTRAQ 116**	**iTRAQ 117**
19748	1	la-sunitinib	sunitin b	mouse brain	CID	iTRAQ	20		VC	
19749	1	la-sunitinib	sunitin b	mouse kidney	CID	iTRAQ		20		VC

Compound profiling experiments on sunitinib matrix: potency of sunitinib and S7; data for Figure 1D												
							compound concentrations [µM]					
experiment ID	**SI data set number**	**probe matrix**	**compound for competition**	**lysate material**	**MS method**	**isobaric tags**	**TMT 126**	**TMT 127**	**TMT 128**	**TMT 129**	**TMT 130**	**TMT 131**
21785	2	la-sunitinib	sunitinib	mouse brain	CID/HCD TDA	TMT	30	7.5	1.875	0.469	0.117	VC
21727	2	la-sunitinib	sunitinib	mouse brain	CID/HCD	TMT	30	7.5	1.875	0.469	0.117	VC
21797	2	la-sunitinib	sunitinib	mouse kidney	CID/HCD	TMT	30	7.5	1.875	0.469	0.117	VC
22592	2	la-sunitinib	sunitinib	mouse kidney	CID/HCD	TMT	30	7.5	1.875	0.469	0.117	VC
21781	2	la-sunitinib	S7	mouse brain	CID/HCD TDA	TMT	30	7.5	1.875	0.469	0.117	VC
22242	2	la-sunitinib	S7	mouse brain	CID/HCD TDA	TMT	30	7.5	1.875	0.469	0.117	VC
22647	2	la-sunitinib	S7	mouse brain	CID/HCD TDA	TMT	30	7.5	1.875	0.469	0.117	VC
22744	2	la-sunitinib	S7	mouse brain	CID/HCD	TMT	30	7.5	1.875	0.469	0.117	VC
21663	2	la-sunitinib	S7	mouse kidney	CID/HCD	TMT	30	7.5	1.875	0.469	0.117	VC
21799	2	la-sunitinib	S7	mouse kidney	CID/HCD	TMT	30	7.5	1.875	0.469	0.117	VC

Compound profiling experiments on la-S7 matrix, potency of CZC-25146 and CZC-54252 against LRRK2 from mouse brain and kidney lysate; data for Table S3 and Figure 2C												
							compound concentrations [µM]					
experiment ID	**SI data set number**	**probe matrix**	**compound for competition**	**lysate material**	**MS method**	**isobaric tags**	**TMT 126**	**TMT 127**	**TMT 128**	**TMT 129**	**TMT 130**	**TMT 131**
20568	3	la-S7	CZC-25146	mouse brain	PQD	TMT	3	0.75	0.188	0.047	0.011	VC
20823	3	la-S7	CZC-25146	mouse brain	PQD	TMT	3	0.75	0.188	0.047	0.011	VC
19704	3	la-S7	CZC-25146	mouse kidney	PQD	TMT	3	0.75	0.188	0.047	0.011	VC
20914	3	la-S7	CZC-25146	mouse kidney	PQD	TMT	3	0.75	0.188	0.047	0.011	VC
20567	3	la-S7	CZC-54252	mouse brain	PQD	TMT	3	0.75	0.188	0.047	0.011	VC
20822	3	la-S7	CZC-54252	mouse brain	PQD	TMT	3	0.75	0.188	0.047	0.011	VC
19703	3	la-S7	CZC-54252	mouse kidney	PQD	TMT	3	0.75	0.188	0.047	0.011	VC
20800	3	la-S7	CZC-54252	mouse kidney	PQD	TMT	3	0.75	0.188	0.047	0.011	VC

Selectivity profiling experiments on Kinobeads matrix against i) HeLa, ii) mixed Jurkat, Ramos and iii) mouse brain lysates; data for Figure 2C and Table S4												
							compound concentrations [µM]					
experiment ID	**SI data set number**	**probe matrix**	**compound for competition**	**lysate material**	**MS method**	**isobaric tags**	**TMT 126**	**TMT 127**	**TMT 128**	**TMT 129**	**TMT 130**	**TMT 131**
21614	4	kinobeads	CZC-25146	mouse brain	CID/HCD TDA	TMT	3	0.75	0.188	0.047	0.011	VC
21957	4	kinobeads	CZC-25146	mouse brain	CID/HCD TDA	TMT	3	0.75	0.188	0.047	0.011	VC
20559	4	kinobeads	CZC-25146	HeLa	CID/HCD TDA	TMT	3	0.75	0.188	0.047	0.011	VC
20818	4	kinobeads	CZC-25146	HeLa	CID/HCD TDA	TMT	3	0.75	0.188	0.047	0.011	VC
21622	4	kinobeads	CZC-25146	Jurkat, Ramos mix	CID/HCD TDA	TMT	3	0.75	0.188	0.047	0.011	VC
21798	4	kinobeads	CZC-25146	Jurkat, Ramos mix	CID/HCD TDA	TMT	3	0.75	0.188	0.047	0.011	VC
21615	4	kinobeads	CZC-54252	mouse brain	CID/HCD TDA	TMT	3	0.75	0.188	0.047	0.011	VC
21956	4	kinobeads	CZC-54252	mouse brain	CID/HCD TDA	TMT	3	0.75	0.188	0.047	0.011	VC
20558	4	kinobeads	CZC-54252	HeLa	CID/HCD TDA	TMT	3	0.75	0.188	0.047	0.011	VC
20817	4	kinobeads	CZC-54252	HeLa	CID/HCD TDA	TMT	3	0.75	0.188	0.047	0.011	VC
21623	4	kinobeads	CZC-54252	Jurkat, Ramos mix	CID/HCD TDA	TMT	3	0.75	0.188	0.047	0.011	VC
23399	4	kinobeads	CZC-54252	Jurkat, Ramos mix	CID/HCD TDA	TMT	10	2.5	0.625	0.156	0.039	VC

Table S2:

Sequence coverage of LRRK2 captured from mouse brain and kidney. Note that sequence coverage suggests that the lower band observed in kidney and other lysates is an N-terminally truncated fragment

Mouse brain	
Sequence coverage from high quality peptides (red; underlined; bold print)	20.1 %
Sequence coverage from all identified peptides (red)	25.4 %

MASGACQGCEEEEEEEALKKLIVRLNNVQEGKQIETLLQLLEDMLVFTYSDRASKLFEDKNFHVPLLIVLDSYMR**VASVQQAGWSLLCK**LIEVCPGTLQS
LIGPQDIGNDWEVLGIHRLILKMLTVHHANVNLSIVGLKALDLLLDSGKLTLLILDEECDIFLLIFDAMHRYSANDEVQKLGCK**ALHVLFER**VSEEQLTE
FVENKDYTILLSTFGSFRRDKEIVYHVLCCLHSLAVTCSNVEVLMSGNVRCYNLVVEAMK**AFPTNENIQEVSCSLFQK**LTLGNFFNILVLNEVHVFVVKA
VRQYPENAALQISALSCLALLTETIFLNQDLEERSETQEQSEEEDSEKLFWLEPCYKALVRHRKDKHVQEAACWALNNLLMYQNSLHEKIGDEDGQFPAH
REVMLSMLMHSSSKDVFQAAAHALSTLLEQNVNFRKILLAK**GVYLNVLELMQK**HAHAPEVAESGCKMLSHLFEGSNPSLDTMAAVVPKILTVMKAHGTSL
SVQLEALR**AILHFVVPGLLEESR**EDSQCRPNVLRKQCFRTDIHK**LVLVALNR**FIGNPGIQKCGLKVISSLAHLPDATETLSLQGAVDSVLHTLQMYPDDQ
EIQCLGLHLMGCLMTKKNFCIGTGHLLAKILASTLQRFKDVAEVQTTGLQTTLSILELSVSFSKLLVHYSFDVVIFHQMSSSVVEQK**DEQFLNLCCK**CFA
K**VAVDDELKNTMLER**ACDQNNSIMVECLLLLGADANQVK**GATSLIYQVCEKESSPKLVELLLNGGCR**EQDVRKALTISIQK**GDSQVISLLLR**KLALDLAN
NSICLGGFGIGK**IDPSWLGPLFPDK**SSNLR**KQTNTGSVLAR**KVLRYQMRNTLQEGVASGSDGNFSEDALAKFGEWTFIPDSSMDSVFGQSDDLDSEGSES
SFLVKR**KSNSISVGEVYR**DLALQRYSPNAQRHSNSLGPVFDHEDLLRRKR**KILSSDESLR**SSRLPSHMR**QSDSSSSLASER**EHITSLDLSANELKDIDAL
SQKCCLSSHLEHLTK**LELHQNSLTSFPQQLCETLK**CLIHLDLHSNK**FTSFPSFVLK**MPRITNLDASRNDIGPTVVLDPAMKCPSLKQLNLSYNQLSSIPE
NLAQVVEKLEQLLLEGNKISGICSPLSLKELK**ILNLSK**NHIPSLPGDFLEACSK**VESFSAR**MNFLAAMPALPSSITSLK**LSQNSFTCIPEAIFSLPHLR**S
LDMSHNNIECLPGPAHWKSLNLR**ELIFSK**NQISTLDFSENPHVWSRVEKLHLSHNKLKEIPPEIGCLENLTSLDVSYNLELRSFPNEMGKLSK**IWDLPLD**
GLHLNFDFKHVGCKAKDIIRFLQQRLKK**AVPYNR**MK**LMIVGNTGSGKTTLLQQLMK**MK**KPELGMQGATVGIDVR**DWSIQIRGKRRKDLVLNVWDFAGREE
FYSTHPHFMTQR**ALYLAVYDLSKGQAEVDAMKPWLFNIK**ARASSSPVILVGTHLDVSDEKQRK**ACISK**ITKELLNKRGFPTIRDYHFVNATEESDALAKL
RK**TIINESLNFK**IRDQPVVGQLIPDCYVELEKIILSERKAVPTEFPVINRKHLLQLVNEHQLQLDENELPHAVHFLNESGVLLHFQDPALQLSDLYFVEP
KWLCK**VMAQILTVK**VDGCLKHPKGIISRRDVEKFLSKKKRFPKNYMMQYFKLLEKFQIALPIGEEYLLVPSSLSDHRPVIELPHCENSEIIIRLYEMPYF
PMGFWSRLINR**LLEISPFMLSGR**ERALRPNRMYWRQGIYLNWSPEAYCLVGSEVLDNRPESFLK**ITVPSCR**KGCILLGRVVDHIDSLMEEWFPGLLEIDI
CGEGETLLKKWALYSFNDGEEHQK**ILLDELMK**KAEEGDLLINPDQP**RLTIPISQIAPDLILADLPR**NIMLNNDELEFEEAPEFLLGDGSFGSVYR**AAYEG**
EEVAVKIFNKHTSLRLLRQELVVLCHLHHPSLISLLAAGIRPR**MLVMELASK**GSLDRLLQQDKASLTRTLQHR**IALHVADGLR**YLHSAMIIYRDLKPHNV
LLFTLYPNAAIIAKIADYGIAQYCCRMGIKTSEGTPGFRAPEVARGNVIYNQQADVYSFGLLLHDIWTTGSRIMEGLRFPNEFDELAIQGKLPDPVKEYG
CAPWPMVEKLITKCLKENPQERPTSAQVFDILNSAELICLMRHILIPKNIIVECMVATNLNSKSATLWLGCGNTEK**GQLSLFDLNTERYSYEEVADSRIL**
CLALVHLAAEKESWVVCGTQSGALLVINVEEETKRHTLEKMTDSVTCLHCNSLAKQSKQSNFLLVGTADGNLMIFEDKAVKCKGAAPLKTLHIGDVSTPL
MCLSESLNSSERHITWGGCGTKVFSFSNDFTIQKLIETKTNQLFSYAAFSDSNIIALAVDTALYIAK**KNSPVVEVWDKK**TEK**LCELIDCVHFLK**EVMVKL
NKESK**HQLSYSGR**VK**ALCLQK**NTALWIGTGGGHILLLDLSTRRVIR**TIHNFCDSVRAMATAQLGSLKNVMLVLGYK**RKSTEGIQEQKEIQSCLSIWDLNL
PHEVQNLEKHIEVRTELADKMRKTSVE

Mouse kidney (upper band)	
Sequence coverage from high quality peptides (red; underlined; bold print)	25.1 %
Sequence coverage from all identified peptides (red)	32.8 %

MASGACQGCEEEEEEEALKKLIVRLNNVQEGKQIETLLQLLEDMLVFTYSDRASKLFEDKNFHVPLLIVLDSYMRVASVQQAGWSLLCKLIEVCPGTLQS
LIGPQDIGNDWEVLGIHRLILKMLTVHHANVNLSIVGLK**ALDLLLDSGK**LTLLILDEECDIFLLIFDAMHR**YSANDEVQK**LGCK**ALHVLFER**VSEEQLTE
FVENKDYTILLSTFGSFRRDKEIVYHVLCCLHSLAVTCSNVEVLMSGNVRCYNLVVEAMKAFPTNENIQEVSCSLFQKLTLGNFFNILVLNEVHVFVVKA
VRQYPENAALQISALSCLALLTETIFLNQDLEER**SETQEQSEEEDSEKLFWLEPCYK**ALVRHRKDKHVQEAACWALNNLLMYQNSLHEK**IGDEDGQFPAH**
REVMLSMLMHSSSKDVFQAAAHALSTLLEQNVNFRKILLAK**GVYLNVLELMQK**HAHAPEVAESGCK**MLSHLFEGSNPSLDTMAAVVPK**ILTVMK**AHGTSL**
SVQLEALRAILHFVVPGLLEESREDSQCRPNVLRKQCFRTDIHK**LVLVALNR**FIGNPGIQKCGLKVISSLAHLPDATETLSLQGAVDSVLHTLQMYPDDQ
EIQCLGLHLMGCLMTK**KNFCIGTGHLLAKILASTLQR**FKDVAEVQTTGLQTTLSILELSVSFSKLLVHYSFDVVIFHQMSSSVVEQK**DEQFLNLCCK**CFA
K**VAVDDELK**NTMLERACDQNNSIMVECLLLLGADANQVK**GATSLIYQVCEK**ESSPK**LVELLLNGGCR**EQDVRKALTISIQK**GDSQVISLLLR**K**LALDLAN**
NSICLGGFGIGKIDPSWLGPLFPDKSSNLR**KQTNTGSVLAR**KVLRYQMRNTLQEGVASGSDGNFSEDALAKFGEWTFIPDSSMDSVFGQSDDLDSEGSES
SFLVKRK**SNSISVGEVYR**DLALQRYSPNAQRHSNSLGPVFDHEDLLRRKR**KILSSDESLR**SSRLPSHMR**QSDSSSSLASER**EHITSLDLSANELKDIDAL
SQKCCLSSHLEHLTKLELHQNSLTSFPQQLCETLKCLIHLDLHSNK**FTSFPSFVLK**MPR**ITNLDASRNDIGPTVVLDPAMK**CPSLKQLNLSYNQLSSIPE
NLAQVVEKLEQLLLEGNK**ISGICSPLSLK**ELK**ILNLSK**NHIPSLPGDFLEACSK**VESFSAR**MNFLAAMPALPSSITSLKLSQNSFTCIPEAIFSLPHLRS

LDMSHNNIECLPGPAHWKSLNLRELIFSKNQISTLDFSENPHVWSRVEKLHLSHNKLKEIPPEIGCLENLTSLDVSYNLELRSFPNEMGKLSKIWDLPLD
GLHLNFDFKHVGCKAKDIIRFLQQRLKKAVPYNRMKLMIVGNTGSGKTTLLQQLMKMKKPELGMQGATVGIDVRDWSIQIRGKRRKDLVLNVWDFAGREE
FYSTHPHFMTQRALYLAVYDLSKGQAEVDAMKPWLFNIKARASSSPVILVGTHLDVSDEKQRKACISKITKELLNKRGFPTIRDYHFVNATEESDALAKL
RKTIINESLNFKIRDQPVVGQLIPDCYVELEKIILSERKAVPTEFPVINRKHLLQLVNEHQLQLDENELPHAVHFLNESGVLLHFQDPALQLSDLYFVEP
KWLCKVMAQILTVKVDGCLKHPKGIISRRDVEKFLSKKKRFPKNYMMQYFKLLEKFQIALPIGEEYLLVPSSLSDHRPVIELPHCENSEIIIRLYEMPYF
PMGFWSRLINRLLEISPFMLSGRERALRPNRMYWRQGIYLNWSPEAYCLVGSEVLDNRPESFLKITVPSCRKGCILLGRVVDHIDSLMEEWFPGLLEIDI
CGEGETLLKKWALYSFNDGEEHQKILLDELMKKAEEGDLLINPDQPRLTIPISQIAPDLILADLPRNIMLNNDELEFEEAPEFLLGDGSFGSVYRAAYEG
EEVAVKIFNKHTSLRLLRQELVVLCHLHHPSLISLLAAGIRPRMLVMELASKGSLDRLLQQDKASLTRTLQHRIALHVADGLRYLHSAMIIYRDLKPHNV
LLFTLYPNAAIIAKIADYGIAQYCCRMGIKTSEGTPGFRAPEVARGNVIYNQQADVYSFGLLLHDIWTTGSRIMEGLRFPNEFDELAIQGKLPDPVKEYG
CAPWPMVEKLITKCLKENPQERPTSAQVFDILNSAELICLMRHILIPKNIIVECMVATNLNSKSATLWLGCGNTEKGQLSLFDLNTERYSYEEVADSRIL
CLALVHLAAEKESWVVCGTQSGALLVINVEEETKRHTLEKMTDSVTCLHCNSLAKQSKQSNFLLVGTADGNLMIFEDKAVKCKGAAPLKTLHIGDVSTPL
MCLSESLNSSERHITWGGCGTKVFSFSNDFTIQKLIETKTNQLFSYAAFSDSNIIALAVDTALYIAKKNSPVVEVWDKKTEKLCELIDCVHFLKEVMVKL
NKESKHQLSYSGRVKALCLQKNTALWIGTGGGHILLLDLSTRRVIRTIHNFCDSVRAMATAQLGSLKNVMLVLGYKRKSTEGIQEQKEIQSCLSIWDLNL
PHEVQNLEKHIEVRTELADKMRKTSVE

Mouse kidney (lower band)	
Sequence coverage from high quality peptides (red; underlined; bold print)	15.0 %
Sequence coverage from all identified peptides (red)	20.0 %

MASGACQGCEEEEEEEALKKLIVRLNNVQEGKQIETLLQLLEDMLVFTYSDRASKLFEDKNFHVPLLIVLDSYMRVASVQQAGWSLLCKLIEVCPGTLQS
LIGPQDIGNDWEVLGIHRLILKMLTVHHANVNLSIVGLKALDLLLDSGKLTLLILDEECDIFLLIFDAMHRYSANDEVQKLGCKALHVLFERVSEEQLTE
FVENKDYTILLSTFGSFRRDKEIVYHVLCCLHSLAVTCSNVEVLMSGNVRCYNLVVEAMKAFPTNENIQEVSCSLFQKLTLGNFFNILVLNEVHVFVVKA
VRQYPENAALQISALSCLALLTETIFLNQDLEERSETQEQSEEEDSEKLFWLEPCYKALVRHRKDKHVQEAACWALNNLLMYQNSLHEKIGDEDGQFPAH
REVMLSMLMHSSSKDVFQAAAHALSTLLEQNVNFRKILLAKGVYLNVLELMQKHAHAPEVAESGCKMLSHLFEGSNPSLDTMAAVVPKILTVMKAHGTSL
SVQLEALRAILHFVVPGLLEESREDSQCRPNVLRKQCFRTDIHKLVLVALNRFIGNPGIQKCGLKVISSLAHLPDATETLSLQGAVDSVLHTLQMYPDDQ
EIQCLGLHLMGCLMTKKNFCIGTGHLLAKILASTLQRFKDVAEVQTTGLQTTLSILELSVSFSKLLVHYSFDVVIFHQMSSSVVEQKDEQFLNLCCKCFA
KVAVDDELKNTMLERACDQNNSIMVECLLLLGADANQVKGATSLIYQVCEKESSPKLVELLLNGGCREQDVRKALTISIQKGDSQVISLLLRKLALDLAN
NSICLGGFGIGKIDPSWLGPLFPDKSSNLRKQTNTGSVLARKVLRYQMRNTLQEGVASGSDGNFSEDALAKFGEWTFIPDSSMDSVFGQSDDLDSEGSES
SFLVKRKSNSISVGEVYRDLALQRYSPNAQRHSNSLGPVFDHEDLLRRKRKILSSDESLRSSRLPSHMRQSDSSSSLASERSEHITSLDLSANELKDIDAL
SQKCCLSSHLEHLTKLELHQNSLTSFPQQLCETLKCLIHLDLHSNKFTSFPSFVLKMPRITNLDASRNDIGPTVVLDPAMKCPSLKQLNLSYNQLSSIPE
NLAQVVEKLEQLLLEGNKISGICSPLSLKELKILNLSKNHIPSLPGDFLEACSKVESFSARMNFLAAMPALPSSITSLKLSQNSFTCIPEAIFSLPHLRS
LDMSHNNIECLPGPAHWKSLNLRELIFSKNQISTLDFSENPHVWSRVEKLHLSHNKLKEIPPEIGCLENLTSLDVSYNLELRSFPNEMGKLSKIWDLPLD
GLHLNFDFKHVGCKAKDIIRFLQQRLKKAVPYNRMKLMIVGNTGSGKTTLLQQLMKMKKPELGMQGATVGIDVRDWSIQIRGKRRKDLVLNVWDFAGREE
FYSTHPHFMTQRALYLAVYDLSKGQAEVDAMKPWLFNIKARASSSPVILVGTHLDVSDEKQRKACISKITKELLNKRGFPTIRDYHFVNATEESDALAKL
RKTIINESLNFKIRDQPVVGQLIPDCYVELEKIILSERKAVPTEFPVINRKHLLQLVNEHQLQLDENELPHAVHFLNESGVLLHFQDPALQLSDLYFVEP
KWLCKVMAQILTVKVDGCLKHPKGIISRRDVEKFLSKKKRFPKNYMMQYFKLLEKFQIALPIGEEYLLVPSSLSDHRPVIELPHCENSEIIIRLYEMPYF
PMGFWSRLINRLLEISPFMLSGRERALRPNRMYWRQGIYLNWSPEAYCLVGSEVLDNRPESFLKITVPSCRKGCILLGRVVDHIDSLMEEWFPGLLEIDI
CGEGETLLKKWALYSFNDGEEHQKILLDELMKKAEEGDLLINPDQPRLTIPISQIAPDLILADLPRNIMLNNDELEFEEAPEFLLGDGSFGSVYRAAYEG
EEVAVKIFNKHTSLRLLRQELVVLCHLHHPSLISLLAAGIRPRMLVMELASKGSLDRLLQQDKASLTRTLQHRIALHVADGLRYLHSAMIIYRDLKPHNV
LLFTLYPNAAIIAKIADYGIAQYCCRMGIKTSEGTPGFRAPEVARGNVIYNQQADVYSFGLLLHDIWTTGSRIMEGLRFPNEFDELAIQGKLPDPVKEYG
CAPWPMVEKLITKCLKENPQERPTSAQVFDILNSAELICLMRHILIPKNIIVECMVATNLNSKSATLWLGCGNTEKGQLSLFDLNTERYSYEEVADSRIL
CLALVHLAAEKESWVVCGTQSGALLVINVEEETKRHTLEKMTDSVTCLHCNSLAKQSKQSNFLLVGTADGNLMIFEDKAVKCKGAAPLKTLHIGDVSTPL
MCLSESLNSSERHITWGGCGTKVFSFSNDFTIQKLIETKTNQLFSYAAFSDSNIIALAVDTALYIAKKNSPVVEVWDKKTEKLCELIDCVHFLKEVMVKL
NKESKHQLSYSGRVKALCLQKNTALWIGTGGGHILLLDLSTRRVIRTIHNFCDSVRAMATAQLGSLKNVMLVLGYKRKSTEGIQEQKEIQSCLSIWDLNL
PHEVQNLEKHIEVRTELADKMRKTSVE

Table S3:

Potency of CZC-25146 and CZC-54252 against LRRK2 from mouse brain and kidney lysate

		Mouse brain		Mouse kidney	
		Quant. MS Experiment 1	Quant. MS Experiment 2	Quant. MS Experiment 1	Quant. MS Experiment 2
IC_{50} [nM]	CZC-25146	23	18	20	24
	CZC-54252	25	28	12	<12

Table S4:

Physicochemical and pharmacokinetic properties of LRRK2 probe compound CZC-25146

A) Physicochemical and *in-vitro* pharmacological properties of CZC-25146

Microsomal stability Clint (mL/min/g liver)	Human	0.472
	Mouse	0.377
CACO-2 permeability Mean papp $x10^6$ cms^{-1}	A to B	23.7
	B to A	39.7
CACO-2	Efflux ratio	1.68
Plasma Protein Binding (% bound in 50% plasma)	Mouse	55.9

B) Pharmacokinetic properties of CZC-25146

	i.v. 1 mg/kg	*p.o.* 5 mg/kg
Cl (L/h/kg)	2.3	
V_{ss} (L/kg)	5.4	
t1/2 (h)	1.6	1
t_{max} (h)	0	0.25
C_{max} (ng/mL)	154	1357
AUC_{last} (h*ng/mL)	419	2878
AUC_{inf} (h*ng/mL)	434	2894
F (%)		133

Following intravenous administration of CZC-25146 to male CD-1 mice at 1 mg/kg body weight, the plasma half life was 1.6 hours, and the clearance rate was 2.3 L/h/kg, which is approximately 43% of the liver blood flow of a typical mouse. The volume of distribution was 5.4 L/kg which is greater than the total body water of a typical mouse, suggesting extensive distribution throughout the body tissues. After oral dosing of 5 mg/kg, CZC-25146 reached maximum plasma concentrations by 0.25 hour post dose. The oral bioavailability was 133%.

The brain-to-plasma ratio of CZC-25146 was evaluated in fasted male CD-1 mice after intravenous dosing at 1 mg/kg. Plasma and brain levels were determined at 1 and 3 h post dose. Atenolol was administered as a control to estimate blood contamination in the excised brain. After intravenous dosing, the average corrected brain to plasma ratio for CZC-25146 was 4.1% ± 0.9% at 1 hour post dose. The brain to plasma ratio could not be determined at 3 h post dose because the brain concentrations were below the limit of quantitation of 1 ng/mL.